ELSEVIER

Thermochimica Acta 317 (1998) 175–182

thermochimica acta

# Thermolytic degradation behavior of inorganic ion-exchanger incorporated Nafion-117

S.K. Tiwari[1,a], S.K. Nema[a], Y.K. Agarwal[b,*]

[a] *Macromolecular Research Center, R.D. University, Jabalpur, 482 001 MP, India*
[b] *School of Science, Gujarat University, Ahmedabad 380 016, Gujarat, India*

Received 7 October 1997; received in revised form 20 April 1998; accepted 22 May 1998

**Abstract**

A perfluoro-sulphonate-ionomer membrane (Nafion-117), incorporated with inorganic ion exchanger (IIE), was evaluated using thermogravimetric analysis and FT-IR spectroscopy to ascertain its thermolytic degradation behavior. The two-step decomposition shown by derivative scans in the Nafion–polyantimonic acid composite was studied by obtaining FT-IR spectra of thermally treated specimens under dynamic conditions up to 200°, 350° and 400°C. Similar studies were carried out for Nafion–zirconium phosphate and Nafion–zirconium oxide composites. Incorporation of IIE invariably decreased the thermal stability of the perfluoro polymer matrix of Nafion. However, the decomposition patterns of $-SO_3H$ groups remained unaffected. Comparative studies of the TGA and DTA scans of these composites show presence of water of crystallization in the incorporated IIEs. © 1998 Elsevier Science B.V.

*Keywords:* Nafion; Polyantimonic acid; Zirconium phosphate; Zirconium oxide; Composite membranes

## 1. Introduction

Ion-exchange membranes have recently acquired great significance owing to their applications in many electrochemical processes [1,2]. Perfluoro-ionomer membranes posses many advantage over other types of membranes, which include excellent chemical, mechanical, and thermal stabilities. The incorporation of electrocatalysts like dispersions of noble metals [3–5], semiconductors [6], and surface modifiers to enhance the hydrophilicity [7] has been accomplished.

In a similar effort, the total ion-exchange capacity (IEC) of Nafion was attempted to be enhanced by the incorporation of inorganic ion exchangers (IIEs). These IIEs have reasonable IECs and were stable towards temperature and ionizing radiations. The choice of IIE depended upon their chemical stability and IEC in different pH environments.

Polyantimonic acid (PAM) was chosen on the basis of its high ion-exchange capacity and good thermal and chemical stability in several hot alkaline and acidic conditions. Membranes for water electrolysis are reported in the literature [8]. They are made by dispersing PAM in the polymeric backbone. IIEs such as zirconium oxide and zirconium phosphate are potential candidates for use in the preparation of inorganic membranes [9,10]. Zirconium oxide behaves as an anion exchanger in acidic and neutral medium and as a cation exchanger in alkaline solutions [11]. Zirconium phosphate in its crystalline state

*Corresponding author.

[1]Present address: ATIRA, P.O. Ambawadi Vistar, Ahmedabad 380 015, Gujarat, India.

0040-6031/98/$19.00 © 1998 Elsevier Science B.V. All rights reserved
*PII* S0040-6031(98)00387-6

of $Zr(HPO_4)_2{\cdot}H_2O$ has two exchangeable hydrogen ions. The protons can be exchanged with alkali-metal ions [12]. Crystalline zirconium phosphate is more stable in alkaline conditions than the amorphous form. Since the electrolysis of water involves highly alkaline conditions, hydrous $ZrO_2$ was chosen as the cation exchanger. Besides imparting ion-exchange functionality, the incorporated ion exchangers were also assumed to behave as fillers or additives. The addition of fillers and additives in plastics is well recognized to impart desired properties such as improvement of strength, fire retardancy and UV resistance [13,14]. Since the method of incorporation of IIEs, which may be regarded as fillers, is different from the conventional procedures, the thermal behavior is expected to change. Further, the proximity of IIE particulates to $-SO_3H$ groups and –COC– linkages may affect the thermal stability of these groups.

The present investigation deals with the thermolysis of IIE incorporated Nafion-117, employing IR spectroscopy and thermal analysis (thermogravimetry, derivative thermogravimetry and differential thermal analysis).

## 2. Experimental

Nafion-117, having equivalent weight of 1100 and thickness of ~180 μm was obtained from E.I. DuPont de Nemours, USA. The membrane was pretreated by boiling in concentrated nitric acid and distilled water (1 : 1) for 30 min followed by rinsing with distilled water. The membrane was subsequently boiled in distilled water for 1 h [15].

Antimony pentachloride ($SbCl_5$) was obtained from Fluka (Switzerland) and was untreated. Aliquots of 6.5% w/v antimony pentachloride solutions were prepared in chloroform (Merck).

Zirconyl oxychloride ($ZrOCl_2{\cdot}8H_2O$) was obtained from Fluka (Switzerland) and was used as supplied. Aliquots of 0.06 M solutions of $ZrOCl_2{\cdot}8H_2O$ were prepared in methanol.

### 2.1. Preparation of polyantimonic acid (PAM) incorporated Nafion

The pretreated samples were converted into $Na^+$ form by keeping them in 0.1 M sodium chloride for 1 h, followed by washing and boiling in distilled water to remove the excess sorbed sodium chloride. The specimens were then vacuum-dried at 110°C for 4 h. The dried films were weighed and again subjected to drying under the aforementioned conditions for another 15 min. The dry specimens were immediately transferred into methanol at 60°C for 5 min and allowed to swell. The methanol swelled films were then transferred to antimony pentachloride solution in chloroform.

While incorporating any IIE, the equilibration with electrolyte was carried out under identical conditions, at 3–5°C, since evaporation of solvent would take place at room temperature, thereby effecting change in concentration. Methanol was the solvent of choice as maximum swelling of Nafion could be achieved [16]. To keep uniform concentrations for all the incorporations, these conditions were adopted throughout. Therefore, methanol-swelled Nafion films were equilibrated with antimony pentachloride solutions in chloroform at 3–5°C. Chloroform was used as solvent to avoid precipitation of $Sb_2O_5$ in the solution because a solution made in methanol may contain water.

After equilibrating for 24 h at 3–5°C, the membrane samples were transferred to a 0.5-M hydrochloric acid solution at 60°C for 4 h to allow the precipitation of PAM. Polyantimonic-acid-incorporated Nafion membranes are designated as Nafion–polyantimonic-acid composite membranes. The amount of PAM in Nafion–polyantimonic acid composite membrane was further increased by repeating the procedure. The percentages of ion exchanger incorporated in each loading are given in brackets.

### 2.2. Preparation of zirconium-phosphate $\{Zr(HPO_4)_2{\cdot}H_2O\}$-incorporated Nafion

The pretreated Nafion samples were kept in 0.06-M zirconyl oxychloride solution at 3–5°C for 24 h. The zirconyl oxychloride sorbed films were then transferred into a round-bottom flask containing 8% *ortho*-phosphoric acid at 60°C and refluxed for 30 min. Formation of zirconium phosphate was indicated as the film turned white. Zirconium-phosphate incorporated membranes are designated as Nafion–zirconium phosphate composite membranes. The amount of zirconium phosphate incorporated in Nafion–zirconium phosphate composite was further increased by

repeating the incorporation procedure. The percent quantity of incorporated zirconium phosphate is shown in brackets.

### 2.3. Preparation of zirconium oxide ($ZrO_2$)-incorporated Nafion

The soaking of Nafion specimens was carried out as explained under the zirconium phosphate composites. The soaked films were subjected to hot boiling 0.1-M $NH_4OH$ aqueous solution for 25 min. The composite was not stable in acidic conditions and, therefore, for further incorporations, the composites were not pretreated. The loadings were increased by keeping the dried samples in zirconlum oxychloride solutions and then treating with warm $NH_4OH$ solution. Zirconium-oxide incorporated membranes are designated as Nafion–zirconium oxide composite membranes and the percent incorporated quantity is similarly shown in brackets.

## 3. Characterization

### 3.1. Thermal analysis

All thermogravimetric analyses were carried out on a Perkin–Elmer TGA (7-Series) equipped with 7700 data station. The rate of heating was 20°C/min with sample purge of nitrogen at 4–6 psi and balance purge at 1–3 psi. DTA studies were carried out on a DuPont thermal analyzer equipped with 2100 control system. The heating rate was a 20°C/min for all analysis.

### 3.2. FT-IR spectroscopic analysis

A Perkin–Elmer 1720 X FT-IR was used for IR spectral data. The range of the FT-IR was 4000–400 $cm^{-1}$ and the resolution was 4 $cm^{-1}$.

To understand various decomposition steps observed in the scans, the composite samples were run on TGA from 40° to 350° and 400°C under nitrogen atmosphere and the heating rate was kept at 20°C/min. The thermally treated samples were subjected to IR analysis to monitor the changes in characteristic spectral bands of perfluoro matrix of Nafion. For the sake of comparison, the control specimen of nafion was also subjected to various thermal treatments and, thereafter, IR evaluation. The ratios of different bands, viz. $–CF_2–$, $–SO_3H$ and –COC– appearing at 1152, 1060 and 984 $cm^{-1}$, respectively, were analyzed to ascertain the decomposition behavior.

X-ray diffraction studies of these composites were carried out to determine the crystal structure [17]. The percentages of incorporated IIEs were determined by a weight differential method, i.e.

$$\text{Percent incorporated IIE} = \frac{W_i - W_v}{W_v} \times 100$$

where, $W_i$ is the weight of IIE incorporated composite membrane, and $W_v$ the weight of virgin Nafion.

## 4. Results and discussion

### 4.1. A. Nafion–polyantimonic-acid composites

The thermal decomposition patterns of Nafion–polyantimonic acid composites are given in Table and 2. The representative thermogravimetry (TG), derivative thermogravimetry (DTG) and differential thermal analysis (DTA) curves of Nafion and Nafion—polyantimonic acid composite (8 : 1) are represented in Figs. 1 and 2, respectively. The DTG curve exhibits two peaks, in the regions 250–350°C and 350–550°C. The DTA curve reveals one broad endotherm from 40–250°C and two exotherms in 250–350° region. While the endotherm indicates the removal of 3–4 water molecules of crystalline polyantimonic acid PAM the two exotherms suggests the decomposition of the polymer matrix (Nafion) composite. The third exotherm (shoulder) in 450–550°C region may be due to the conversion of $Sb_2O_5$ to $Sb_6O_{13}$ [18].

The thermogravimetry, derivative thermogravimetry and differential thermal analysis curves of virgin Nafion show a nominal weight loss in the 300-400°C region which was suggested to be due to the loss of $–SO_3H$ groups [19]. On comparison, the first exotherm of the composite, which falls in the same region is conspicuous by its appearance and represents higher weight losses that can be justified by assuming the partial loss of the hydrocarbon backbone in Nafion along with $–SO_3H$ groups.

In order to ascertain the degradation behavior of the Nafion–polyantimonic acid composite, the composites

Table 1
Thermal characteristic data of various composite membranes

| Composite | Decomposition | | | | | |
|---|---|---|---|---|---|---|
| | 1st Step | | 2nd Step | | 3rd Step | |
| | maxima | assignment | maxima | assignment | maxima | assignment |
| Nafion | 350°C | $SO_3H$+COC (partial) | 410°C | $SO_3H$+COC (complete) | 490°C | fluorocarbon matrix |
| NAF PAM (8.1) | 300°C | $SO_3H$+COC+$CF_2$ | 370°C | $SO_3H$+COC+$H_2O$ with PAM | 450°C | fluorocarbon matrix |
| NAF PAM (31.2) | 280°C | $SO_3H$+COC+$CF_2$ (partial) | | | 440°C | $SO_3H$+COC+$CF_2$ (complete) |
| NAF PAM (39.7) | 275°C | $SO_3H$+COC+$CF_2$ (partial) | | | 420°C | $SO_3H$+COC+$CF_2$ (complete) |
| NAF ZRP (36.6) | 320°C | interstitial $H_2O$ with ZrP+$SO_3H$+COC+$CF_2$ | 400°C | $SO_3H$+COC | 490°C | Fluorocarbon matrix |
| NAF ZRP (46.4) | 290°C | -do- | 390°C | $SO_3H$+COC | 440°C | flurocarbon matrix |
| NAF ZRP (64.7) | 290°C | -do- | | | 420°C | flurocarbon matrix |
| NAF ZRO (9.6) | 300°C | $SO_3H$+COC+$CF_2$ (partial) | | | 470°C | fluorocarbon matrix (complete) |
| NAF ZRO (14.1) | 300°C | $SO_3H$+COC+$CF_2$ (partial) | | | 460°C | fluorocarbon matrix (complete) |
| NAF ZRO (16.2) | 300°C | $SO_3H$+COC+$CF_2$ (partial) | | | 460°C | fluorocarbon matrix (complete) |

Table 2
Decomposition patterns of various composite membranes

| Composite | Onset of decomposition/°C | | | Weight loss of polymer matrix/% | | |
|---|---|---|---|---|---|---|
| | 1st | 2nd | 3rd | 1st | 2nd | 3rd |
| NAFION | 300 | 400 | 420 | 7 | 5 | 88 |
| NAF PAM (8.1) | 250 | 350 | 380 | 16 | 22 | 62 |
| NAF PAM (31.2) | 220 | — | 350 | 22 | — | 78 |
| NAF PAM (39.7) | 210 | — | 340 | 23 | — | 77 |
| NAF ZRP (36.6) | 280 | 340 | 430 | 13 | 23 | 64 |
| NAF ZRP (46.2) | 250 | 325 | 410 | 15 | 30 | 55 |
| NAF ZRP (64.7) | 250 | — | 325 | 16 | — | 84 |
| NAF ZRO (9.6) | 280 | — | 350 | 17 | — | 83 |
| NAF ZRO (14.1) | 280 | — | 340 | 35 | — | 65 |
| NAF ZRO (16.2) | 280 | — | 340 | 42 | — | 58 |

vis-à-vis neat Nafion were subjected to thermal treatment in TGA as explained in the experimental section. The resulting mass was subjected to IR spectrophotometric estimations. Ratios of areas of various characteristic peaks of Nafion and PAM were obtained and are given in Table 3.

The percent weight of –$SO_3H$ and –COC– groups were calculated from the structural formula of Nafion [19] which turns out to be ≈11%. It was further noted that Nafion consisted of three regions; (a) fluorocarbon, (b) interfacial zone, and (c) ionic clusters [16]. The weight percent of the chains present in (b) and (c) regions was calculated to be ≈40%.

Barring the loss of free water, no loss of polymer matrix was observed up to 350°C in the case of unmodified Nafion. This could be substantiated by considering –$CF_2$– group as an internal standard. It may be considered that the thermal stability of –$CF_2$– is very high as is associated with PTFE and, therefore, this group will remain unaffected at this temperature.

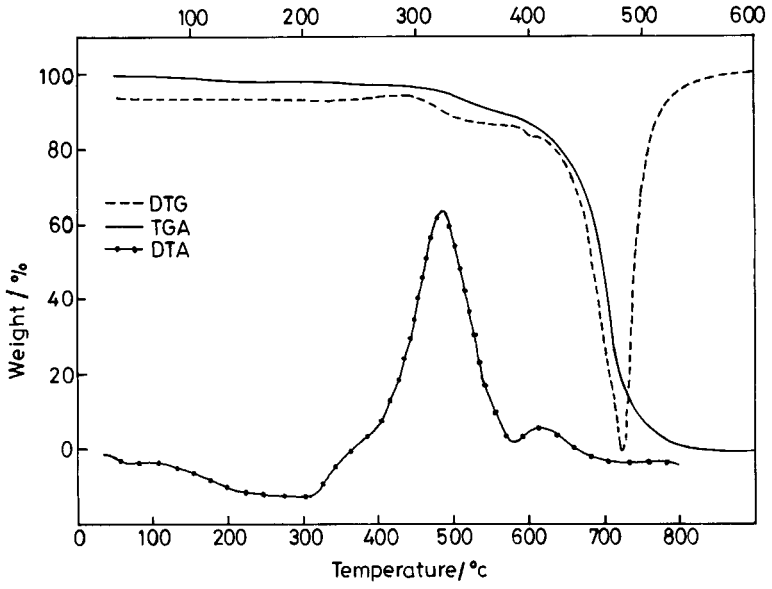


Fig. 1. Derivative thermogravimetry, thermogravimetry and differential thermal analysis curves of Nafion.

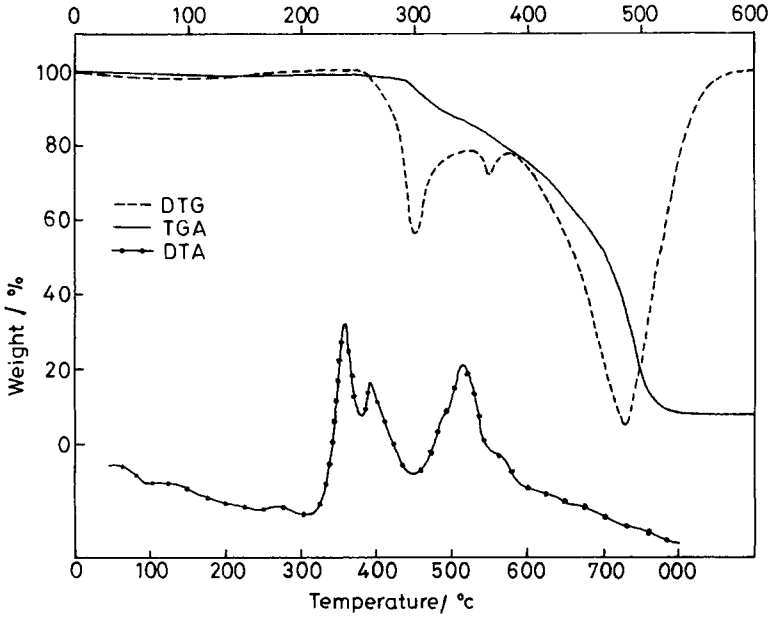


Fig. 2. Derivative thermo grvimetry, thermogravimetry and differential thermal analysis curves of NAF PAM (8.1) composite.

As no observable loss of polymer matrix was seen up to 350°C, the peak area ratios of various groups of neat Nafion with respect to its $-CF_2-$ group (350°C) were taken as the reference.

The ratios obtained for Nafion–polyantimonic acid composites suggest the decomposition of Nafion matrix which probably would be as the loss of the B and C regions of Nafion. It may further be inferred

Table 3
Ratios of different peak areas after thermal treatments at 350° and 400°C

| Composite | Treatment (°C) | $SO_3H/CF_2$ | $COC/CF_2$ | $SO_3H/COC$ |
|---|---|---|---|---|
| NAFION | 350 | 0.82 | 0.81 | 1.04 |
| | 400 | 0.80 | 0.75 | 1.08 |
| NAF PAM (8.1) | 350 | 0.82 | 0.79 | 1.04 |
| | 400 | 0.75 | 0.70 | 1.12 |
| NAF PAM (31.2) | 350 | 0.74 | 0.74 | 1.00 |
| | 400 | 0.53 | 0.51 | 1.04 |
| NAF PAM (39.7) | 350 | 0.71 | 0.74 | 0.96 |
| | 400 | 0.52 | 0.50 | 1.04 |
| NAF ZRO (9.6) | 350 | 0.77 | 0.76 | 1.01 |
| | 400 | 0.01 | — | — |
| NAF ZRO (14.1) | 350 | 0.74 | 0.75 | 0.99 |
| | 400 | — | — | — |
| NAF ZRO (16.2) | 350 | 0.73 | 0.73 | 1.00 |
| | 400 | 0.01 | — | — |

that the presence of IIE has a catalytic effect on decomposition of Nafion.

From DTG and DTA curves, it is further observed that there is a gradual shift in the first- and third-step decomposition towards lower temperatures. It may also be observed from maxima the Tables 1 and 2 that the second decomposition step is absent because of the early onset of the third decomposition step. This observation suggests that incorporation of PAM catalyzes the decomposition of Nafion matrix.

### *4.2. B. Nafion–zirconium phosphate composites*

The representative thermogravimetry, derivative thermogravimetry and differential thermal analysis curves of Nafion–zirconium phosphate (36.6) composite are shown in Fig. 3. The DTG curves show a three-step decomposition. The first step occurred in the 250–350°C region while the second step occurred in the 350–450°C region. The third step, which occurred in the 450–550°C region, involved the maximum weight loss.

DTA curves show a broad endotherm accompanied by one weak and one strong and broad exotherm. The endotherm suggests the loss of three crystallographically different water molecules [20] attached to α-zirconium phosphate. FT-IR studies of thermally treated samples further substantiate this view owing to the disappearance of vibrational frequencies of free water molecules at 3756 ($\nu_3$), 3652 ($\nu_1$) and 1595 ($\nu_2$) $cm^{-1}$. The second weight loss can be suggested to be due to

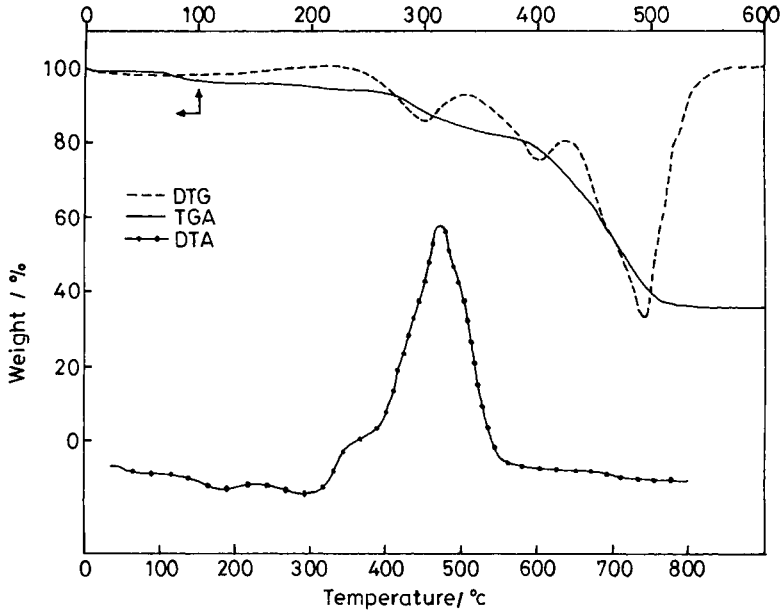


Fig. 3. Derivative thermogravimetry, thermogravimetry and differential thermal analysis curves of NAF ZRP (36.6) composite.

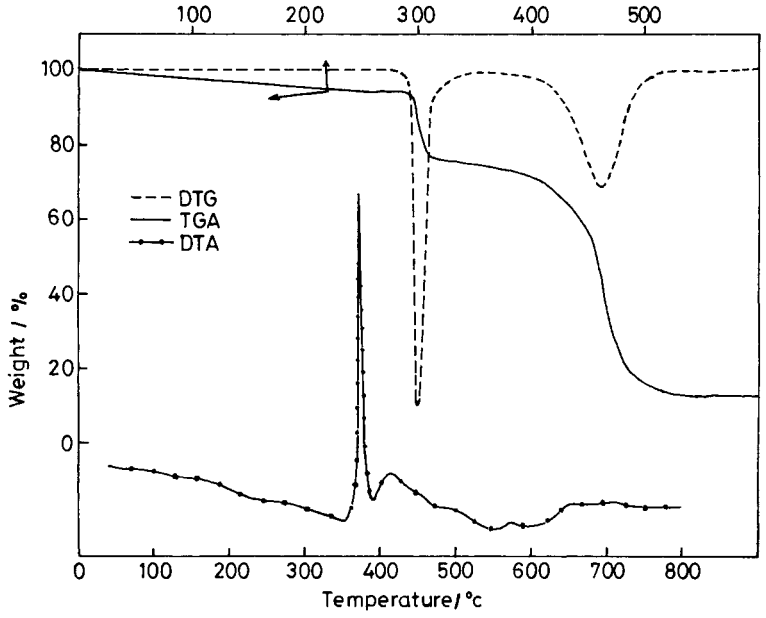


Fig. 4. Derivative thermogravimetry and differential thermal analysis curves of NAF ZRO (14.1) composite.

the decomposition of $-SO_3H$ groups along with fluorocarbon backbone of Nafion.

The identification of the moieties responsible for weight losses at various temperatures was difficult as the absorption bands of incorporated zirconium phosphate in the Nafion were very strong in the region where most of the characteristic peaks of Nafion occur, i.e. 1300–900 $cm^{-1}$.

A gradual shift in decomposition maxima (derivative thermogravimetry) towards lower temperatures with increase of incorporated zirconium phosphate can be observed from Table 1. This may be attributed to the catalytic effect of incorporated zirconium phosphate on the decomposition of Nafion.

### *4.3. C. Nafion–zirconium-oxide composites*

Fig. 4 represents the thermogravimetry, derivative thermogravimetry and differential thermal analysis curves of Nafion–zirconium-oxide (14.1) composite. The thermal decomposition pattern can be observed from Tables 1 and 2. A two-step decomposition of Nafion matrix could be seen from the DTG curve. The first step occurred in the 250–350°C region. However, it was much sharper in comparison to that observed in the other two types of composites. This step may be due to the partial decomposition of the Nafion matrix. DTA curves showed two exotherms, the first being very strong and sharp. The endotherm representing the loss of water was practically absent, thus indicating very small quantities of water in the composites. The studies to determine water contents have also revealed the presence of very low quantities of water [17].

IR spectra were unable to provide much information regarding the weight loss during the first step of thermal decomposition as weak bands of zirconium oxide were completely overlapped by strong vibration bands of Nafion. The high weight loss, however, can only be attributed to the decomposition of the Nafion matrix which includes all three groups.

An almost complete loss of $-SO_3H$ and –COC– groups was observed for the samples treated up to 400°C. Comparatively speaking, the IR spectra of Nafion–polyantimonic acid composites showed presence of weak bands of the $-SO_3H$ and –COC– groups. This finding suggests faster decomposition of these groups in zirconium-oxide incorporated Nafion.

From Tables 1 and 2 it is evident that the onset and decomposition maxima of polymer matrix is gradually shifted towards lower temperatures with increase in

incorporated zirconium oxide content. This also indicates the catalytic effect of incorporated zirconium oxide on decomposition on Nafion matrix.

## 5. Conclusions

It may be concluded that all types of composites show a gradual decrease in decomposition temperatures contradictory to the view which suggests increase in decomposition temperatures by addition of fillers and additives. Incompatibility of IIEs with the polymer may be the reason to this effect.

## References

[1] W.G.F. Grot, G.E. Munn, P.N. Welmsley, 141st National Meeting of Electrochemical Society, Houston, TX, May 1972.
[2] R.S. Yeo, J. McBreen, G. Kissel, F. Kulesa, S. Srinivasan, J. Appl. Electrochem. 10 (1980) 741.
[3] P. Millet, M. Pineri, R. Durand, J. Appl. Electrochem. 19 (1989) 162.
[4] P. Millet, R. Durand, M. Pineri, Int. J. Hydrogen Energy 15 (1990) 245.
[5] H. Tanaka, E. Torikai, Jap. Kokai Tokkyo Koho 8038934.
[6] M. Krishnan, J.R. White, M.A. Fox, A.J. Bard, J. Am. Chem. Soc. 105 (1983) 7002.
[7] Asahi Glass Co. Ltd., European Patent Application 61 594.
[8] H. Vandenborre, R. Leysen, H. Nackaerts, D. Vander Eeken, Ph. Van Asbroeck, W. Smets, J. Piepers, Int. J. Hydrogen Energy 10 (1985) 719.
[9] G. Alberti, Atti. Accad. Naz. Lincei, Rend. Classe Sci. Fis. Mat. Nat. 31 (1961) 427.
[10] G. Alberti, M. Casciola, U. Costantino, G. Levi, J. Membr. Sci. 3 (1978) 179.
[11] C.B. Amphlett, L.A. McDonald, M.J. Redman, J. Inorg. Nucl. Chem. 6 (1958) 236.
[12] F. Mounier, L. Winand, Bull. Soc. Chim. Fr. (1968) 1829.
[13] G.R. Moore, D.I. Kline, in: Properties and Processing of Polymers for Engineers, Society of Plastic Engineers, Prentice-Hall Inc., Englewood Cliffs, NJ, 1984.
[14] Encyclopedia of Polymer Science & Engineering, vol. 3 & 7, IInd edn., Wiley-Interscience, 1985.
[15] A.W.-H. Mau, C.-B. Huang, N. Kakuta, A.J. Bard, A. Campion, M.A. Fox, J.M. White, S.E. Webber, J. Am. Chem. Soc. 106 (1984) 6537.
[16] A. Eisenberg, H.L. Yeager (Ed.), Perfluorinated lonomer Membranes. ACS Symposium Series, 180, American Chemical Society, Washington DC, 1982.
[17] S.K. Tiwari, Ph.D. Thesis, MRC, R.D. University, Jabalpur, 1995.
[18] M. Abe, Kogyo Kogaku Zasshi 70 (1967) 2226.
[19] J. Surowiec, R. Bogoczek, J. Therm. Anal. 33 (1988) 1097.
[20] S.E. Horsley, D.V. Nowell, D.T. Stewart, Spectrochim. Acta 30A (1974) 535.